

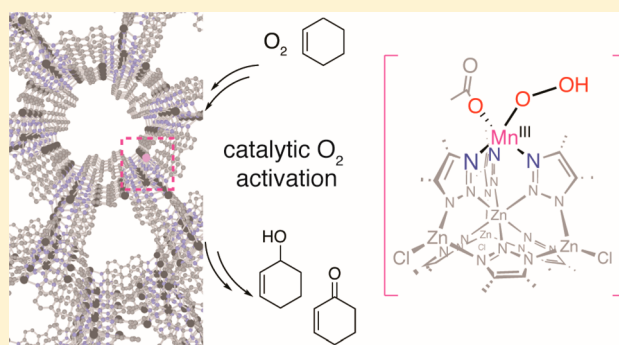
# Selective Oxidation of C–H Bonds through a Manganese(III) Hydroperoxo in Mn<sup>II</sup>-Exchanged CFA-1

Amanda W. Stubbs<sup>1</sup> and Mircea Dinca<sup>1\*</sup>

Department of Chemistry, Massachusetts Institute of Technology, 77 Massachusetts Avenue, Cambridge, Massachusetts 02139, United States

## Supporting Information

**ABSTRACT:** Partial substitution of Zn<sup>II</sup> by Mn<sup>II</sup> in Zn<sub>5</sub>(OAc)<sub>4</sub>(S,S'-bibenzo[d][1,2,3]triazole)<sub>3</sub> (CFA-1) results in a Mn<sup>II</sup> species supported by three nitrogen ligands and a charge-balancing anion, a structure reminiscent of those found in molecular “scorpionate” complexes. Unlike molecular manganese(II) scorpionates, Mn-CFA-1 is capable of catalytically activating oxygen from air to oxidize C–H bonds up to 87 kcal/mol in strength. A series of in situ spectroscopic studies, including diffuse-reflectance UV–vis, diffuse-reflectance infrared Fourier transform spectroscopy, and X-ray absorption spectroscopy, reveal that catalysis likely proceeds through a manganese(III) hydroperoxo that is only accessed in the presence of a hydrogen-atom donor. These results demonstrate that the site isolation provided in metal–organic frameworks enables the generation and utilization of highly reactive species for catalysis that are inaccessible in molecular systems.



## INTRODUCTION

Selective oxidations are key steps in the transformation of both petroleum and biofeedstocks into commodity chemicals and ultimately into consumer products. Often, oxidations are achieved with the intermediacy of reactive metal oxo species, which typically suffer either from indiscriminate reactivity and a lack of selectivity toward a range of C–H bonds or from bimolecular decomposition.<sup>1–4</sup> Manganese is an element of interest for these transformations because of its prevalence in biological transformations involving oxygen-atom transfer and the ease of access to multiple redox states.<sup>5–8</sup> However, manganese-based molecular catalysts are particularly prone to bimolecular decomposition, while most *isolated* molecular examples of manganese(IV) oxo species display sluggish oxygen-atom-transfer reactivity, at least, in part, because of the strongly donating ligand fields and steric bulk typically required for their isolation.<sup>9–11</sup>

Metal–organic frameworks (MOFs) confer several advantages for heterogeneous small-molecule chemistry, lending such attributes as ease of product separation and site isolation, coupled with well-defined, tunable catalytic sites.<sup>12–15</sup> The combination of these features enables access to unique coordination geometries around metal ions that are otherwise inaccessible in molecular analogues and sometimes lead to unusual reactivity.<sup>16,17</sup> The carboxylate and azolate binding moieties that often serve as the node-to-linker interface in MOFs offer relatively weak ligand fields, especially compared to those found in the ligands of molecular manganese complexes. These weaker ligand fields combined with site

isolation make it possible to access and utilize highly reactive metal–oxygen species.<sup>18</sup>

Here, we took inspiration from a family of molecular manganese complexes colloquially known as “scorpionates”, which feature manganese–oxygen species that are primed for reactivity.<sup>19,20</sup> Indeed, several molecular scorpionate-based manganese(III) peroxy species have been isolated, albeit through harsh oxidizing agents such as hydrogen peroxide or potassium superoxide.<sup>21–23</sup> No catalysis has been reported with these species, presumably either because they are sterically accessible but plagued by instability or because they are relatively stable but sterically inaccessible. We surmised that the incorporation of such species within scorpionate-like MOFs would unlock the reactivity potential that has not yet been achieved with molecular manganese scorpionates. This approach is inspired by earlier work wherein Kuratowski clusters in materials such as Zn<sub>5</sub>Cl<sub>4</sub>(BTDD)<sub>3</sub> (MFU-4l)<sup>24</sup> and Zn<sub>5</sub>(OAc)<sub>4</sub>(bibta)<sub>3</sub> (CFA-1)<sup>25</sup> serve as excellent platforms for site-isolated scorpionate chemistry.<sup>26–33</sup> The secondary building units (SBUs) in both of these materials offer metal sites supported by three nitrogen ligands and a charge-balancing anion, comprising a ligand field that is far weaker than those typically reported for known molecular manganese(IV) oxo species.<sup>25</sup> Altogether, these properties make CFA-1, made from a more accessible ligand than MFU-4l, a particularly attractive platform for the isolation of reactive

Received: July 10, 2019

high-valent manganese–oxygen species potentially capable of selective catalytic C–H activation chemistry.

## RESULTS AND DISCUSSION

Mn-CFA-1 (Figure 1) can be accessed via cation exchange at room temperature by gently stirring CFA-1, a crystalline

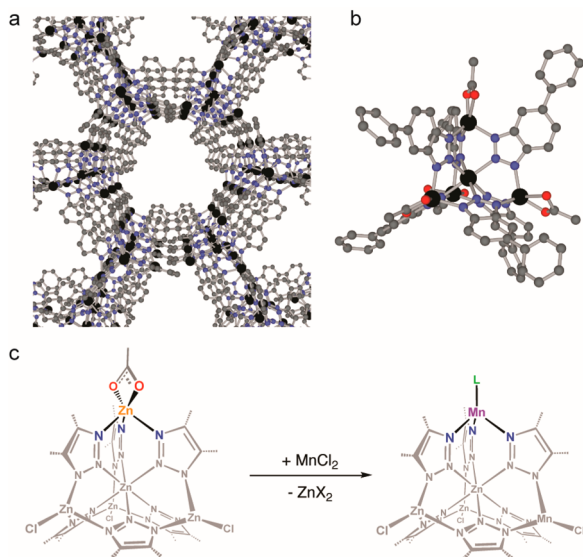


**Figure 1.** (a) Pore structure of CFA-1 (hydrogen atoms and acetate anions omitted for clarity) (b) SBU of CFA-1 (c) schematic of cation exchange reaction in CFA-1

powder, with 50 equiv of  $\text{MnCl}_2 \cdot 4\text{H}_2\text{O}$  in *N,N*-dimethylformamide (DMF) for 7 days. Thorough washing of the solid material isolated from this reaction with DMF and methanol, followed by activation under dynamic vacuum at 180 °C, yields a crystalline material with a Brunauer–Emmett–Teller (BET) surface area of 1990  $\text{m}^2/\text{g}$ , consistent with that of the CFA-1 starting material (see the Supporting Information).<sup>25</sup> Analysis by inductively coupled plasma optical emission spectrometry (ICP-OES) indicates the incorporation of two manganese atoms per SBU, and the  $^1\text{H}$  NMR of an acid-digested material revealed the presence of some residual acetate anions.

A comparison of the X-ray absorption near-edge spectroscopy (XANES) features collected on the activated material sealed in a capillary under an inert atmosphere to  $\text{Mn}^{\text{II}}$  reference compounds indicated that the manganese present in Mn-CFA-1 is in the 2+ formal oxidation state (Figure 2). Exposure of activated Mn-CFA-1 to air for several hours led to only a slight shift in the edge energy (+0.2 eV) relative to pristine Mn-CFA-1 and is indicative of the coordination of a small amount of water to  $\text{Mn}^{\text{II}}$  rather than oxidation to  $\text{Mn}^{\text{III}}$  or higher. Indeed, formal oxidation would be expected to shift the edge energy by several electronvolts, as evidenced by  $\text{Mn}^{\text{III}}$  standards such as  $\text{Mn}_2\text{O}_3$  and  $\text{Mn}(\text{OAc})_3$  (Figure 2).

The first signs of intriguing reactivity of the manganese scorpionate moieties in Mn-CFA-1 came from stoichiometric oxidations of substrates such as cyclohexene to products including cyclohexen-1-ol, cyclohexen-1-one, and cyclohexene oxide using a variety of oxidants including *tert*-butylsulfonyl-2-iodosylbenzene and *tert*-butyl hydroperoxide. The more remarkable reactivity was observed, however, when using air as the terminal oxidant, which led to catalytic and selective formation of alcohol and ketone products from a variety of

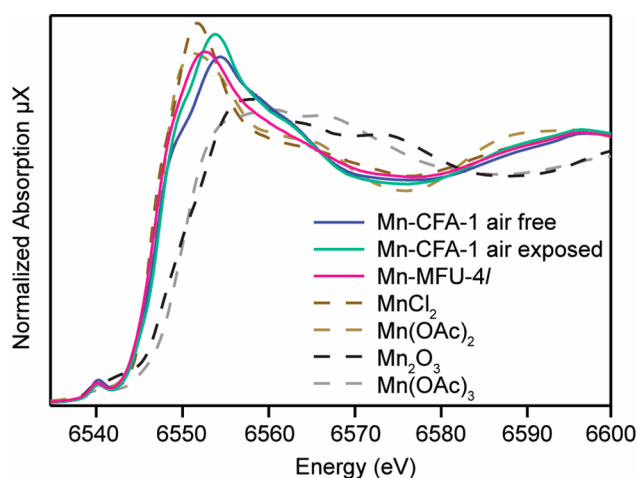


**Figure 2.** XANES data for Mn-MOFs compared with manganese standards.

substrates including ethylbenzene, cyclohexene, cumene, and 1-hexene but not including substrates with stronger C–H bonds such as toluene and cyclohexane. Evidencing the key role of manganese in this reactivity and the heterogeneity of the manganese catalytic site, all-zinc CFA-1 does not enable catalysis under identical conditions, while ICP-OES of a postcatalysis filtrate sample presented no detectable manganese traces in solution. Additionally, powder X-ray diffraction (PXRD) of the solid material postcatalysis indicated good crystallinity that was unchanged from that of the Mn-CFA-1 starting material (Figure S1), eliminating the possibility of framework decomposition.

The heterogeneous nature of the catalysis was further confirmed by a size-exclusion experiment. Thus, Mn-CFA-1 was found to catalyze oxidation of 1,3,5-triisopropylbenzene for a total of 3.3 turnovers per manganese, whereas cumene oxidation was 2.5 times more efficient, with 8.3 turnovers per manganese. It is expected that both of these substrates have comparable benzylic C–H bond strengths; however, cumene at its narrowest width is approximately 4.2 Å, while the narrowest width of 1,3,5-triisopropylbenzene is approximately 7.3 Å. The channels of CFA-1 are only 6.2 Å at their widest aperture. Presumably, whereas cumene is able to diffuse through the pores of the material and undergo oxidation catalyzed by the site-isolated manganese species within, 1,3,5-triisopropylbenzene is likely only able to access manganese species on the surface of the MOF crystals, resulting in more limited conversion. These results are in line with previous observations of size-selective catalysis with MOFs.<sup>18,34–40</sup>

Because of the previously mentioned observation of acetate upon acid digestion of Mn-CFA-1, the impact of the charge-balancing anion identity on catalysis was investigated. Attempts at performing cation exchange on CFA-1 with  $\text{Mn}(\text{OAc})_2 \cdot 4\text{H}_2\text{O}$ , which would theoretically yield a material featuring only acetate anions, were unsuccessful. Additionally, attempts at complete anion exchange of acetate for chloride in Mn-CFA-1 resulted in a poorly crystalline material with severely lowered surface area. Fortunately, the pentanuclear zinc cluster that is the SBU of CFA-1 is a motif that can be found in other MOFs as well, most notably MFU-4l. The latter is isolated with chloride as the charge-balancing anion rather than acetate, thus ensuring that the manganese-exchanged material will feature chloride as the only charge-balancing anion. It has been

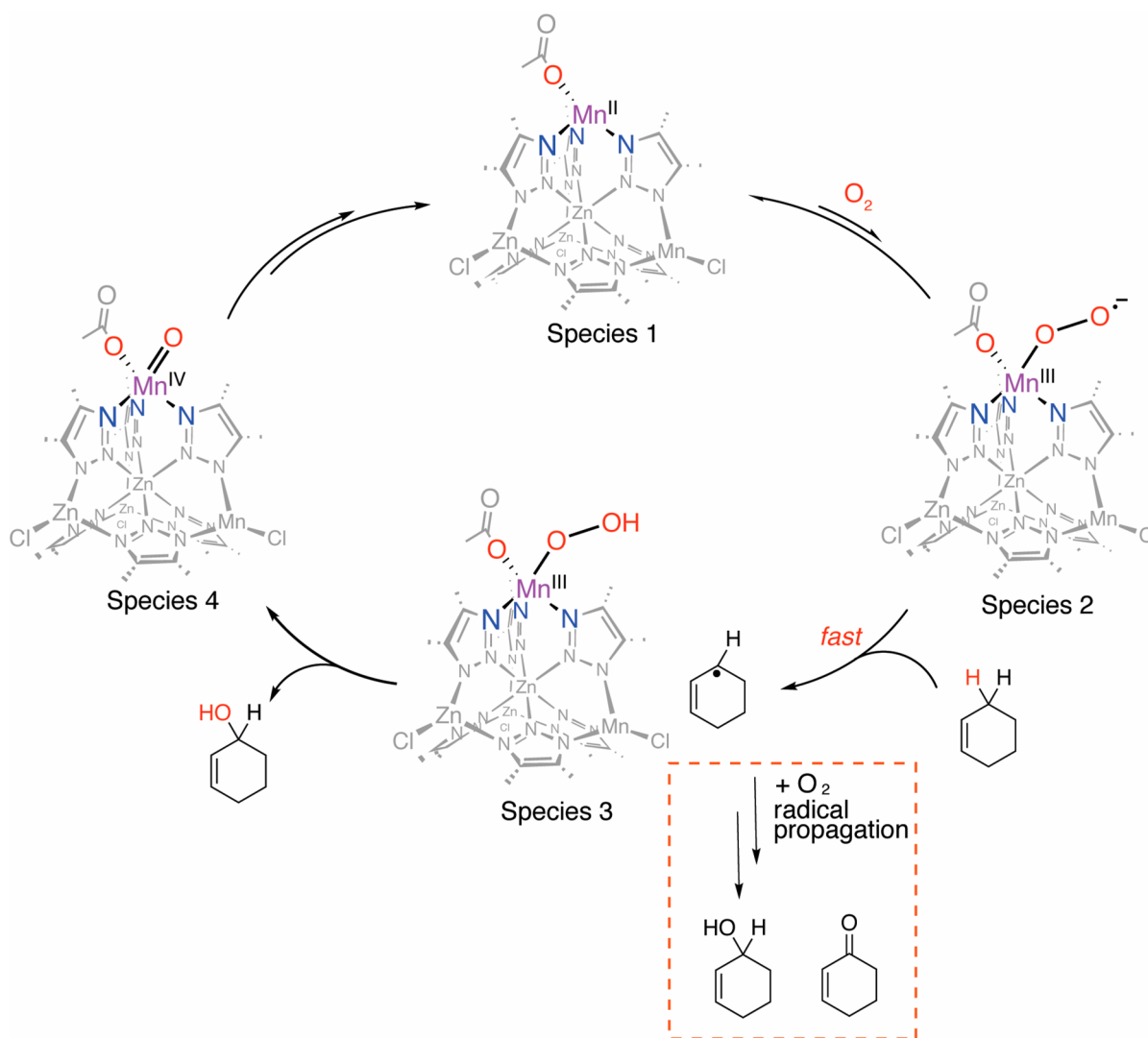
Table 1. Effect of Catalyst, Oxidant, and Reaction Time on the Total Catalyst TON and Selectivity<sup>a</sup>

catalyst	oxidant	time	TON		sum of the alcohol and ketone products	ratio of alcohol/ketone
			alcohol <sup>b</sup>	ketone <sup>c</sup>		
Mn-CFA-1	air	15 min	2.8	3.2	6	1:1.1
Mn-CFA-1	air	1 h	3.8	5.0	8.8	1:1.3
Mn-CFA-1	air	6 h	3.8	6.9	10.7	1:1.8
Mn-CFA-1	O <sub>2</sub> (2 bar)	18 h	5.4	15.8	21.2	1:2.9
Mn-MFU-4l	air	18 h	0.9	0.5	1.4	1:0.55
Mn(CO <sub>2</sub> CH <sub>3</sub> )-MFU-4l	air	18 h	4.7	14.7	19.4	1:1.3
Mn(CO <sub>2</sub> CF <sub>3</sub> )-MFU-4l	air	18 h	5.5	11.1	16.6	1:2.0

<sup>a</sup>Typical reaction conditions: 10 mg of MOF, 1 mL of cyclohexene, 22 °C. <sup>b</sup>Turnovers of cyclohexen-1-ol calculated with respect to manganese.

<sup>c</sup>Turnovers of cyclohexen-1-one calculated with respect to manganese.

Scheme 1. Proposed Catalytic Cycle for Oxidation of Cyclohexene by Mn-CFA-1 in Air



previously reported that highly sensitive catalysis, such as ethylene dimerization to selectively yield 1-butene, proceeds identically in both the CFA-1 and MFU-4l platforms;<sup>27</sup> given their remarkably similar geometries, this was expected to be the case for the oxidation reactions discussed in this work as well. Thus, Mn-MFU-4l was synthesized in a manner similar to that described for Mn-CFA-1 and slightly modified from what has been previously reported.<sup>29</sup> MFU-4l was gently stirred in a DMF solution containing 50 equiv of MnCl<sub>2</sub>·4H<sub>2</sub>O for 7 days.

The solid material isolated from this reaction was washed thoroughly with DMF and methanol and then activated under a high vacuum at 180 °C until a pressure of 10<sup>-5</sup> Torr was achieved. This procedure yielded a high-quality material with good crystallinity and a BET surface area of 3570 m<sup>2</sup>/g, consistent with that of the MFU-4l starting material and with the value previously reported for Mn-MFU-4l. ICP-OES analysis indicated the incorporation of 1.8 manganese atoms per SBU, and the <sup>1</sup>H NMR of the acid-digested material

confirmed that, indeed, no acetate anions were present. Extended X-ray absorption fine structure (EXAFS) analysis was performed on this material and yielded a fit consistent with the substitution of manganese for zinc into the MOF framework, complete with a charge-balancing chloride anion. Details of this analysis can be found in the [Supporting Information](#).

Tellingly, for the influence of the anion on reactivity, Mn-MFU-4l, which is never exposed to acetate, does not catalyze the oxidation of cyclohexene with air, with the reactivity observed being merely stoichiometric ([Table 1](#)). Subjecting Mn-MFU-4l to a sodium acetate solution yields Mn(CO<sub>2</sub>CH<sub>3</sub>)-MFU-4l, a material with good crystallinity where 2.7 chlorides per SBU are replaced by acetates (see the [Supporting Information](#)). This acetate-exchanged Mn-MFU-4l does enable catalytic oxidation of cyclohexene in the presence of air, conclusively demonstrating the critical role of acetate for oxidation activity by manganese in both Mn-CFA-1 and Mn-MFU-4l. Adding a large excess of sodium acetate to Mn-CFA-1 did not significantly increase the number of turnovers for cyclohexene oxidation, suggesting that acetate is not consumed in the reaction, but rather facilitated it as a ligand on the manganese. Importantly, replacing even only 0.9 of the chloride anions in each SBU of MFU-4l by trifluoroacetate produces a material, Mn(CO<sub>2</sub>CF<sub>3</sub>)-MFU-4l (see the [Supporting Information](#)), that is as active as Mn-MFU-4l with a more significant acetate content, underscoring the importance of weak ligand-field anions in promoting oxidation catalysis with manganese-substituted Kuratowski clusters.

Visual inspection of the reaction progress provides first clues to the potential mechanism of O<sub>2</sub> activation and reactivity with the manganese-exchanged MOFs. Thus, when substrates with sufficiently weak C–H bonds are added to beige Mn-CFA-1 in air, the MOF turns black upon contact and then rapidly lightens to dark brown over the course of 5 min; as the reaction continues overnight, the material returns to its original color. This series of color changes is not observed when the substrate is introduced to Mn-CFA-1 in the absence of oxygen, nor is it ever observed when the substrate has C–H bonds that are too strong to be oxidized, such as toluene. These visual observations combined with the decline in catalyst performance over time suggest that a highly reactive species forms initially only in the presence of both O<sub>2</sub> and substrate and that this species is responsible for the majority of the observed reactivity, before disappearing from the reaction mixture. A plausible scenario is one where, in the presence of a suitable hydrogen-atom donor, manganese(III) hydroperoxo is formed and kicks off the catalytic cycle shown in [Scheme 1](#). Although rare, the few manganese(III) hydroperoxo species reported in the literature are accessed in a similar manner: a Mn<sup>II</sup> complex is oxidized by molecular oxygen in the presence of a hydrogen-atom donor to yield manganese(III) hydroperoxo, presumably via a very transient manganese(III) superoxo.<sup>41,42</sup> In support of this hypothesis, the addition of only 10 equiv of benzoquinone per manganese, a well-known superoxide and hydroperoxide scavenger,<sup>34,43</sup> results in a more than 60% reduction in the oxidized product produced by Mn-CFA-1 in air. Although the proposed manganese(III) hydroperoxo was not isolable in our hands, we assign its relative instability to the comparatively weaker ligand field conferred by Mn-CFA-1 relative to those in reported manganese(III) hydroperoxo molecular species. Notably, the same reasoning explains the increased reactivity of the putative manganese(III) superoxo here, which is able to

oxidize stronger C–H bonds than previously seen with molecular systems.

In line with our qualitative visual observations, in situ spectroscopic experiments confirmed oxidation of Mn<sup>II</sup> in Mn-CFA-1 as well as changes in its electronic structure upon exposure to cyclohexene in air. Although Mn<sup>II</sup>-CFA-1 in air has no strong absorptions in diffuse-reflectance (DR) UV–vis ([Figure 3a](#)), new absorptions at 439 and 650 nm appear upon

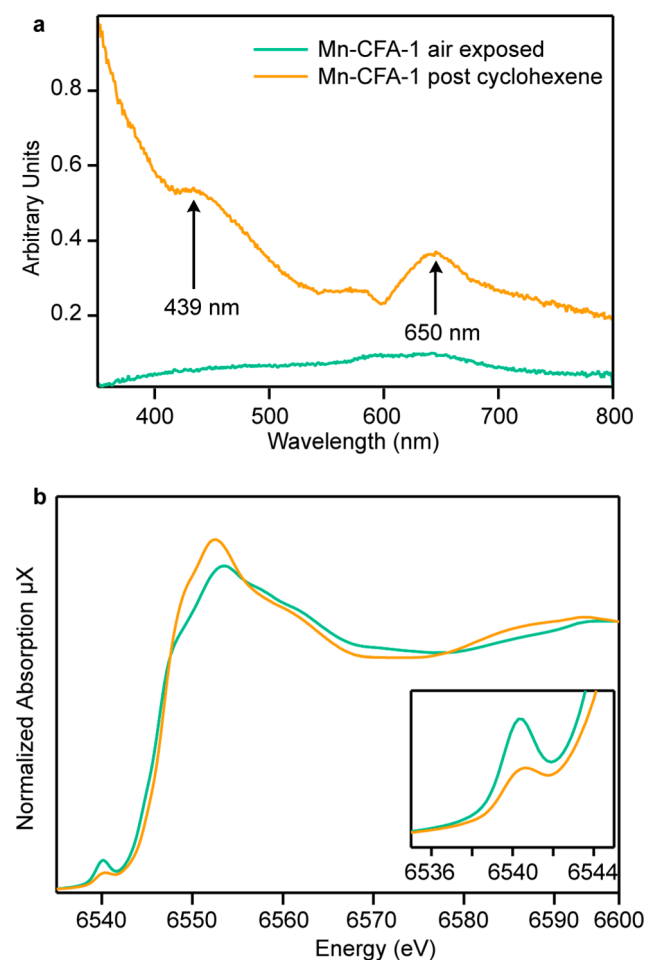


**Figure 3.** (a) DR UV–vis and (b) XANES data of Mn-CFA-1 in air, before and after exposure to cyclohexene.

the addition of 1 drop of cyclohexene. These bands are not associated with pure cyclohexene itself and likely indicate the formation of Mn<sup>III</sup>, wherein d–d transitions become spin-allowed.

In situ XANES measurements provided more conclusive evidence for the formation of Mn<sup>III</sup> upon exposure of Mn-CFA-1 to both cyclohexene and air. Thus, whereas exposing Mn-CFA-1 to a flow of simulated air (20% O<sub>2</sub> in N<sub>2</sub>) produced no visible changes in the XAS spectrum, adding cyclohexene to the in situ gas flow caused an abrupt change in the edge energy and line shape ([Figure 3b](#)). More specifically, a shift in the edge energy of +0.5 eV and a shift of the pre-edge feature by +0.3 eV were consistent with the oxidation of manganese. Although not as dramatic as those observed for molecular manganese scorpionates undergoing oxidation from Mn<sup>II</sup> to Mn<sup>III</sup>,<sup>23</sup> we note that the Mn<sup>III</sup> in our system is likely not a dominant species when the system reaches the steady state. Indeed, in light of the catalytic cycle proposed in [Scheme 1](#), we

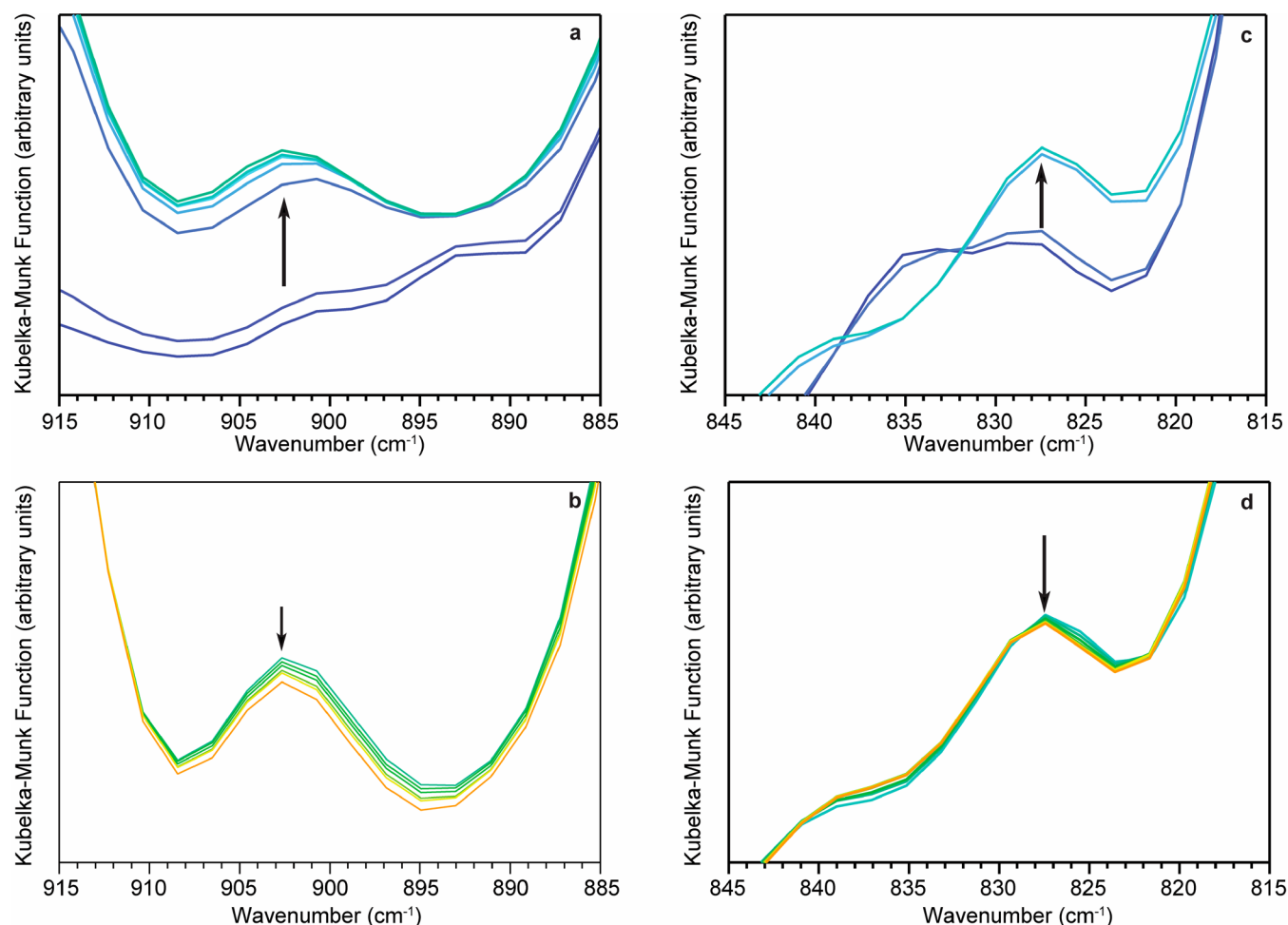


**Figure 4.** In situ DRIFTS of Mn-CFA-1 after exposure to O<sub>2</sub> and cyclohexene. Spectra were collected over the course of 15 min; a feature at 903 cm<sup>-1</sup> grows in (a) and then diminishes (b), as does a feature at 827 cm<sup>-1</sup>, which also grows in (c) and then diminishes (d)

do not anticipate that 100% of the manganese in the sample would be oxidized from Mn<sup>II</sup> at any given point in time. Of even greater interest is the decrease in the intensity of the preedge feature at 6540.3 eV upon exposure to cyclohexene. The preedge features of Mn-XANES spectra are closely related to the symmetry at the manganese site<sup>44,45</sup> and here suggest that the manganese site reaches a more centrosymmetric environment upon exposure to air and cyclohexene, resulting in a less intense preedge feature. This would be in line with the manganese atom gaining another ligand (such as the hydroperoxo).

Additional evidence for the formation of manganese(III) hydroperoxo came from in situ diffuse-reflectance infrared Fourier transform spectroscopy (DRIFTS; Figure 4). Exposing Mn-CFA-1 to a 10 s “pulse” of O<sub>2</sub> flowing through a saturator filled with cyclohexene caused the appearance of a band at 903 cm<sup>-1</sup> over the course of 20 min, which then gradually disappeared. This frequency is in the region of the O–O bond stretch of the putative hydroperoxo species, as numerous manganese(III) side-on peroxo, manganese(III) hydroperoxo, and manganese(III) alkylperoxo species have been reported in the same region.<sup>21–23,41,46,47</sup> One other band of interest that exhibits the same transient behavior as that at 903 cm<sup>-1</sup> (that is, it grows in and then disappears over the course of approximately 20 min) is 827 cm<sup>-1</sup>. Intriguingly, this frequency is most in line with those of terminal manganese(IV) oxo

species. Although such species are extremely rare, one reported instance for the Mn–O stretching frequency in a manganese(IV) oxo places it at 845 cm<sup>-1</sup>.<sup>48,49</sup>

Although the Mn-CFA-1 and Mn-MFU-4l systems allow the identification of rare, transient manganese(III) hydroperoxo and potentially of a manganese(IV) oxo species with notable reactivity toward C–H bonds, the catalytic activity of these high-valent manganese species is quickly quenched by water formed during the reaction. The appearance of water is readily discernible through in situ DRIFTS experiments (Figure S5). Even increasing the availability of the oxidant by performing the reaction under 2 bar of O<sub>2</sub> and increasing the duration to 18 h did not result in more than a marginal increase in the catalytic performance (Table 1). This is also consistent with the only transient appearance of spectroscopic signatures of Mn<sup>III</sup>-OOH and manganese(IV) oxo that are not discernible beyond the first 30 min of the reaction. Indeed, it is highly likely that the proposed catalytic cycle is only in effect initially, and further turnovers achieved after the inaugural few rounds of catalysis are instead the result of radical processes. Indeed, the addition of 10 equiv of 2,4,6-tri-*tert*-butylphenol, a free-radical scavenger that is too large to diffuse into the pore of Mn-CFA-1, to the reaction inhibits conversion of cyclohexene to oxidized products and, interestingly, keeps the product distribution closer to 1:1 for reactions run for longer than 1 h (Table 2).

**Table 2. Effect of the Free-Radical Inhibitor 2,4,6-Tri-*tert*-butylphenol and Reaction Time on the Total Catalyst TON and Selectivity<sup>a</sup>**

catalyst	oxidant	addition of a free-radical inhibitor <sup>b</sup>	time	TON		sum of the alcohol and ketone products	alcohol/ketone ratio
				alcohol <sup>c</sup>	ketone <sup>d</sup>		
Mn-CFA-1	air	no	1 h	3.8	5.0	8.8	1:1.3
Mn-CFA-1	air	yes	1 h	0.4	0.5	0.9	1:1.3
Mn-CFA-1	air	no	6 h	3.8	6.9	10.7	1:1.8
Mn-CFA-1	air	yes	6 h	1.4	1.6	3	1:1.1

<sup>a</sup>Typical reaction conditions: 10 mg of MOF, 1 mL of cyclohexene, 22 °C. <sup>b</sup>10 equiv of 2,4,6-tri-*tert*-butylphenol. <sup>c</sup>Turnovers of cyclohexen-1-ol calculated with respect to manganese. <sup>d</sup>Turnovers of cyclohexen-1-one calculated with respect to manganese.

The detrimental effect of water on catalysis is made obvious when water is added directly to Mn-CFA-1 prior to the addition of cyclohexene, which reduces product formation by 75%. Although clearly a limitation in batch processes, the generation of reaction-limiting water in situ could be mitigated by implementing catalysis in a flow system. In a setup where all products (desired and otherwise) are swept out of the catalyst bed before having a chance to further react, Mn-CFA-1 could exhibit increased turnover numbers (TONs) for olefin oxidation and potentially increased selectivity. Indeed, a time point study indicated that the bulk of the observed activity for Mn-CFA-1 occurs within the first 15 min of the reaction. Even during this time, the selectivity shifts from an initial alcohol/ketone ratio of approximately 1:1 to the favoring of ketone products over alcohol products as the reaction progresses. The implementation of a flow approach employing Mn-CFA-1 is ongoing.

## CONCLUSION

The foregoing results highlight how the site isolation and relatively weak ligand fields generally exhibited by MOFs, here exemplified by CFA-1, enable the activation of O<sub>2</sub> by a Mn<sup>II</sup> species in a scorpionate environment, followed by reactivity that has not been accessible in molecular systems. Mn-CFA-1 is capable of catalytically oxidizing weak C–H bonds using air as the terminal oxidant with the proposed intermediacy of Mn<sup>III</sup>-OOH. The data provide evidence that this catalysis is influenced by the identity of the charge-balancing anion, and preliminary results suggest that more weakly coordinating species, such as trifluoroacetate, promote even greater catalytic activity. The reaction is inhibited by the inherent formation of water as a side product, likely because of the highly reactive nature of the intermediates in our proposed catalytic cycle, making this catalyst an intriguing candidate for continuous-flow chemistry.

## ASSOCIATED CONTENT

### Supporting Information

The Supporting Information is available free of charge on the ACS Publications website at DOI: 10.1021/acs.inorgchem.9b02068.

Details of experimental procedures and results, PXRD data, nitrogen isotherm data, and EXAFS analysis (PDF)

## AUTHOR INFORMATION

### Corresponding Author

\*E-mail: mdinca@mit.edu.

### ORCID

Amanda W. Stubbs: 0000-0002-5539-273X

Mircea Dinca: 0000-0002-1262-1264

## Author Contributions

The manuscript was written through contributions of all authors. All authors have given approval to the final version of the manuscript.

## Notes

The authors declare no competing financial interest.

## ACKNOWLEDGMENTS

Fundamental studies of cation-exchange and small-molecule interactions with MOFs are supported by the National Science Foundation through a CAREER award to M.D. (Award DMR-1452612). A.W.S. gratefully acknowledges the National Science Foundation Graduate Research Fellowship program for financial support under Grant 1122374. This work made use of the Shared Experimental Facilities supported, in part, by the MRSEC Program of the National Science Foundation under Award DMR-1419807. XAS data collection was done at the NSLS II, a U.S. Department of Energy (DOE), Office of Science User Facility, operated for the U.S. DOE, Office of Science, by Brookhaven National Laboratory under Contract DE-SC0012704. The authors are grateful to Eli Stavitski of the NSLS II ISS Beamline (8-ID) for his expertise in XAS data collection and advice in its workup. A.W.S. is grateful to Dr. Ashley Wright for helpful discussions about oxidation catalysis.

## REFERENCES

- Centi, G.; Cavani, F.; Trifirò, F. Trends and Outlook in Selective Oxidation: An Introduction. In *Selective Oxidation by Heterogeneous Catalysis*; Springer: New York, 2001.
- Labinger, J. A.; Bercaw, J. E. Understanding and Exploiting C-H Bond Activation. *Nature* **2002**, *417*, 507–514.
- Werpy, T.; Petersen, G. Top Value Added Chemicals from Biomass Volume I—Results of Screening for Potential Candidates from Sugars and Synthesis Gas. Technical Report, 2004; DOI: 10.2172/15008859.
- Kuwahara, Y.; Yoshimura, Y.; Yamashita, H. In Situ-Created Mn(III) Complexes Active for Liquid-Phase Oxidation of Alkylaromatics to Aromatic Ketones with Molecular Oxygen. *Catal. Sci. Technol.* **2016**, *6* (2), 442–448.
- Umena, Y.; Kawakami, K.; Shen, J. R.; Kamiya, N. Crystal Structure of Oxygen-Evolving Photosystem II at a Resolution of 1.9 Å. *Nature* **2011**, *473* (7345), 55–60.
- Barynin, V. V.; Whittaker, M. M.; Antonyuk, S. V.; Lamzin, V. S.; Harrison, P. M.; Artymiuk, P. J.; Whittaker, J. W. Crystal Structure of Manganese Catalase from *Lactobacillus Plantarum*. *Structure* **2001**, *9* (8), 725–738.
- Perry, J. J. P.; Shin, D. S.; Getzoff, E. D.; Tainer, J. A. The Structural Biochemistry of the Superoxide Dismutases. *Biochim. Biophys. Acta, Proteins Proteomics* **2010**, *1804* (2), 245–262.
- Wennman, A.; Oliw, E. H.; Karkehabadi, S.; Chen, Y. Crystal Structure of Manganese Lipoyxygenase of the Rice Blast Fungus *Magnaporthe Oryzae*. *J. Biol. Chem.* **2016**, *291* (15), 8130–8139.

- (9) Barman, P.; Vardhaman, A. K.; Martin, B.; Wörner, S. J.; Sastri, C. V.; Comba, P. Influence of Ligand Architecture on Oxidation Reactions by High-Valent Nonheme Manganese Oxo Complexes Using Water as a Source of Oxygen. *Angew. Chem., Int. Ed.* **2015**, *54*, 2095–2099.
- (10) Wu, X.; Seo, M. S.; Davis, K. M.; Lee, Y.-M.; Chen, J.; Cho, K.-B.; Pushkar, Y. N.; Nam, W. A Highly Reactive Mononuclear Non-Heme Manganese(IV)-Oxo Complex That Can Activate the Strong C-H Bonds of Alkanes. *J. Am. Chem. Soc.* **2011**, *133*, 20088–20091.
- (11) Yoon, J.; Seo, M. S.; Kim, Y.; Kim, S. J.; Yoon, S.; Jang, H. G.; Nam, W. Synthesis and Reactivity of a Mononuclear Manganese(II) Complex Having Pseudo-Seven Coordination Environment. *Bull. Korean Chem. Soc.* **2009**, *30* (3), 679–682.
- (12) Dhakshinamoorthy, A.; Asiri, A. M.; Garcia, H. Metal-Organic Frameworks as Catalysts for Oxidation Reactions. *Chem. - Eur. J.* **2016**, *22*, 8012–8024.
- (13) Gascon, J.; Corma, A.; Kapteijn, F.; Llabrés i Xamena, F. X. Metal Organic Framework Catalysis: Quo Vadis? *ACS Catal.* **2014**, *4*, 361–378.
- (14) Chughtai, A. H.; Ahmad, N.; Younus, H. A.; Laypkov, A.; Verpoort, F. Metal-Organic Frameworks: Versatile Heterogeneous Catalysts for Efficient Catalytic Organic Transformations. *Chem. Soc. Rev.* **2015**, *44*, 6804–6849.
- (15) Furukawa, H.; Cordova, K. E.; O’Keeffe, M.; Yaghi, O. M. The Chemistry and Applications of Metal-Organic Frameworks. *Science* **2013**, *341*, 1230444-1–1230444-12.
- (16) Phan, A.; Czaja, A. U.; Gándara, F.; Knobler, C. B.; Yaghi, O. M. Metal-Organic Frameworks of Vanadium as Catalysts for Conversion of Methane to Acetic Acid. *Inorg. Chem.* **2011**, *50* (16), 7388–7390.
- (17) Brozek, C. K.; Miller, J. T.; Stoian, S. A.; Dincă, M. NO Disproportionation at a Mononuclear Site-Isolated Fe(II) Center in Fe(II)-MOF-5. *J. Am. Chem. Soc.* **2015**, *137*, 7495–7501.
- (18) Stubbs, A. W.; Braglia, L.; Borfecchia, E.; Meyer, R. J.; Román-Leshkov, Y.; Lamberti, C.; Dincă, M. Selective Catalytic Olefin Epoxidation with Mn<sup>II</sup>-Exchanged MOF-5. *ACS Catal.* **2018**, *8* (1), 596–601.
- (19) Pettinari, C. Scorpionates: Pinch and Sting. The Metal. *La Chim. L’Industria* **2004**, *10* (86), 94–100.
- (20) Trofimenko, S. *Scorpionates The Coordination Chemistry of Polypyrazolylborate Ligands*; Imperial College Press: London, 1999.
- (21) Kitajima, N.; Komatsuzaki, H.; Hikichi, S.; Osawa, M.; Moro-Oka, Y. A Monomeric Side-On Peroxo Manganese(III) Complex: Mn(O<sub>2</sub>)(3,5-*i*Pr<sub>2</sub> pzH)(HB(3,5-*i*Pr<sub>2</sub> pz)<sub>3</sub>). *J. Am. Chem. Soc.* **1994**, *116* (25), 11596–11597.
- (22) Singh, U. P.; Sharma, A. K.; Hikichi, S.; Komatsuzaki, H.; Moro-Oka, Y.; Akita, M. Hydrogen Bonding Interaction between Imidazolyl N-H Group and Peroxide: Stabilization of Mn(III)-Peroxo Complex Tp<sup>iPr<sub>2</sub></sup>Mn(H<sub>2</sub>O<sub>2</sub>)(Im<sup>MeH</sup>)(ImMeH = 2-Methylimidazole). *Inorg. Chim. Acta* **2006**, *359* (13), 4407–4411.
- (23) Colmer, H. E.; Geiger, R. A.; Leto, D. F.; Wijeratne, G. B.; Day, V. W.; Jackson, T. A. Geometric and Electronic Structure of a Peroxomanganese(III) Complex Supported by a Scorpionate Ligand. *Dalt. Trans.* **2014**, *43* (48), 17949–17963.
- (24) Denysenko, D.; Grzywa, M.; Tonigold, M.; Streppel, B.; Krljus, I.; Hirscher, M.; Mugnaioli, E.; Kolb, U.; Hanss, J.; Volkmer, D. Elucidating Gating Effects for Hydrogen Sorption in MFU-4-Type Triazolate-Based Metal-Organic Frameworks Featuring Different Pore Sizes. *Chem. - Eur. J.* **2011**, *17* (6), 1837–1848.
- (25) Schmieder, P.; Denysenko, D.; Grzywa, M.; Baumgärtner, B.; Senkovska, I.; Kaskel, S.; Sastre, G.; van Wüllen, L.; Volkmer, D. CFA-1: The First Chiral Metal-Organic Framework Containing Kuratowski-Type Secondary Building Units. *Dalt. Trans.* **2013**, *42* (30), 10786.
- (26) Metzger, E. D.; Brozek, C. K.; Comito, R. J.; Dincă, M. Selective Dimerization of Ethylene to 1-Butene with a Porous Catalyst. *ACS Cent. Sci.* **2016**, *2* (3), 148–153.
- (27) Metzger, E. D.; Comito, R. J.; Wu, Z.; Zhang, G.; Dubey, R. C.; Xu, W.; Miller, J. T.; Dincă, M. Highly Selective Heterogeneous Ethylene Dimerization with a Scalable and Chemically Robust MOF Catalyst. *ACS Sustainable Chem. Eng.* **2019**, *7* (7), 6654–666.
- (28) Denysenko, D.; Grzywa, M.; Jelic, J.; Reuter, K.; Volkmer, D. Scorpionate-Type Coordination in MFU-4l Metal-Organic Frameworks: Small-Molecule Binding and Activation upon the Thermally Activated Formation of Open Metal Sites. *Angew. Chem., Int. Ed.* **2014**, *53* (23), 5832–5836.
- (29) Denysenko, D.; Jelic, J.; Reuter, K.; Volkmer, D. Postsynthetic Metal and Ligand Exchange in MFU-4l: A Screening Approach toward Functional Metal-Organic Frameworks Comprising Single-Site Active Centers. *Chem. - Eur. J.* **2015**, *21* (22), 8188–8199.
- (30) Wang, L.; Agnew, D. W.; Yu, X.; Figueroa, J. S.; Cohen, S. M. A Metal-Organic Framework with Exceptional Activity for C-H Bond Amination. *Angew. Chem., Int. Ed.* **2018**, *57* (2), 511–515.
- (31) Dubey, R. J. C.; Comito, R. J.; Wu, Z.; Zhang, G.; Rieth, A. J.; Hendon, C. H.; Miller, J. T.; Dincă, M. Highly Stereoselective Heterogeneous Diene Polymerization by Co-MFU-4l: A Single-Site Catalyst Prepared by Cation Exchange. *J. Am. Chem. Soc.* **2017**, *139* (36), 12664–12669.
- (32) Comito, R. J.; Wu, Z.; Zhang, G.; Lawrence, J. A.; Korzyński, M. D.; Kehl, J. A.; Miller, J. T.; Dincă, M. Stabilized Vanadium Catalyst for Olefin Polymerization by Site Isolation in a Metal-Organic Framework. *Angew. Chem., Int. Ed.* **2018**, *57* (27), 8135–8139.
- (33) Comito, R. J.; Metzger, E. D.; Wu, Z.; Zhang, G.; Hendon, C. H.; Miller, J. T.; Dincă, M. Selective Dimerization of Propylene with Ni-MFU-4l. *Organometallics* **2017**, *36* (9), 1681–1683.
- (34) Santiago-Portillo, A.; Navalón, S.; Cirujano, F. G.; Xamena, F. X. L. I.; Alvaro, M.; Garcia, H. MIL-101 as Reusable Solid Catalyst for Autoxidation of Benzylic Hydrocarbons in the Absence of Additional Oxidizing Reagents. *ACS Catal.* **2015**, *5* (6), 3216–3224.
- (35) Horike, S.; Dincă, M.; Tamaki, K.; Long, J. R. Size-Selective Lewis Acid Catalysis in a Microporous Metal-Organic Framework with Exposed Mn 2+ Coordination Sites. *J. Am. Chem. Soc.* **2008**, *130* (18), 5854–5855.
- (36) Dybtsev, D. N.; Nuzhdin, A. L.; Chun, H.; Bryliakov, K. P.; Talsi, E. P.; Fedin, V. P.; Kim, K. A Homochiral Metal-Organic Material with Permanent Porosity, Enantioselective Sorption Properties, and Catalytic Activity. *Angew. Chem., Int. Ed.* **2006**, *45* (6), 916–920.
- (37) Hasegawa, S.; Horike, S.; Matsuda, R.; Furukawa, S.; Mochizuki, K.; Kinoshita, Y.; Kitagawa, S. Three-Dimensional Porous Coordination Polymer Functionalized with Amide Groups Based on Tridentate Ligand: Selective Sorption and Catalysis. *J. Am. Chem. Soc.* **2007**, *129* (9), 2607–2614.
- (38) Cho, S.-H.; Ma, B.; Nguyen, S. T.; Hupp, J. T.; Albrecht-Schmitt, T. E. A Metal-Organic Framework Material That Functions as an Enantioselective Catalyst for Olefin Epoxidation. *Chem. Commun.* **2006**, No. 24, 2563–2565.
- (39) Lee, D. H.; Kim, S.; Hyun, M. Y.; Hong, J.-Y.; Huh, S.; Kim, C.; Lee, S. J. Controlled Growth of Narrowly Dispersed Nanosize Hexagonal MOF Rods from Mn(III)-Porphyrin and In(NO<sub>3</sub>)<sub>3</sub> and Their Application in Olefin Oxidation. *Chem. Commun.* **2012**, *48* (44), 5512.
- (40) Xie, M.-H.; Yang, X.-L.; He, Y.; Zhang, J.; Chen, B.; Wu, C.-D. Highly Efficient C-H Oxidative Activation by a Porous Mn<sup>III</sup>-Porphyrin Metal-Organic Framework under Mild Conditions. *Chem. - Eur. J.* **2013**, *19* (42), 14316–14321.
- (41) Shook, R. L.; Gunderson, W. A.; Greaves, J.; Ziller, J. W.; Hendrich, M. P.; Borovik, A. S. A Monomeric Mn(III)-Peroxo Complex Derived Directly from Dioxygen. *J. Am. Chem. Soc.* **2008**, *130* (28), 8888–8889.
- (42) Sankaralingam, M.; Lee, Y.; Jeon, S. H.; Seo, M. S.; Cho, K.-B.; Nam, W. A Mononuclear Manganese(III)-Hydroperoxo Complex: Synthesis by Activating Dioxygen and Reactivity in Electrophilic and Nucleophilic Reactions. *Chem. Commun.* **2018**, *54* (54), 1209–1212.
- (43) Manring, L. E.; Kramer, M. K.; Foote, C. S. Interception of O<sub>2</sub>-by Benzoquinone in Cyanoaromatic-Sensitized Photooxygenations. *Tetrahedron Lett.* **1984**, *25* (24), 2523–2526.

(44) Farges, F. Ab Initio and Experimental Pre-Edge Investigations of the Mn K -Edge XANES in Oxide-Type Materials. *Phys. Rev. B: Condens. Matter Mater. Phys.* **2005**, *71* (15), 155109.

(45) Chalmin, E.; Farges, F.; Brown, G. E. A Pre-Edge Analysis of Mn K-Edge XANES Spectra to Help Determine the Speciation of Manganese in Minerals and Glasses. *Contrib. Mineral. Petrol.* **2009**, *157* (1), 111–126.

(46) Coggins, M. K.; Martin-Diaconescu, V.; Debeer, S.; Kovacs, J. a. Correlation between Structural, Spectroscopic, and Reactivity Properties within a Series of Structurally Analogous Metastable Manganese-(III)-Alkylperoxo Complexes. *J. Am. Chem. Soc.* **2013**, *135* (11), 4260–4272.

(47) Parham, J. D.; Wijeratne, G. B.; Rice, D. B.; Jackson, T. A. Spectroscopic and Structural Characterization of Mn(III)-Alkylperoxo Complexes Supported by Pentadentate Amide-Containing Ligands. *Inorg. Chem.* **2018**, *57* (5), 2489–2502.

(48) Halbach, R. L.; Gygi, D.; Bloch, E. D.; Anderson, B. L.; Nocera, D. G. Structurally Characterized Terminal Manganese(IV)-Oxo Tris(Alkoxide) Complex. *Chem. Sci.* **2018**, *9* (19), 4524–4528.

(49) Hong, S.; Lee, Y.-M.; Sankaralingam, M.; Vardhaman, A. K.; Park, Y. J.; Cho, K.-B.; Ogura, T.; Sarangi, R.; Fukuzumi, S.; Nam, W. A Manganese(V)-Oxo Complex: Synthesis by Dioxygen Activation and Enhancement of Its Oxidizing Power by Binding Scandium Ion. *J. Am. Chem. Soc.* **2016**, *138* (27), 8523–8532.